Available online at www.sciencedirect.com

ScienceDirect

Nuclear and Particle Physics Proceedings 273–275 (2016) 2427–2429

www.elsevier.com/locate/nppp

Search for dark photon production at *BABAR*

Bertrand Echenard
On behalf of the *BABAR* Collaboration

California Institute of Technology, Pasadena, California 91125, USA

Abstract

We present a search for a dark photon, a new massive vector boson interacting weakly with Standard Model particles, using data collected with the *BABAR* detector. No statistically significant deviations from the Standard Model predictions are seen, and 90% confidence level upper limits on the mixing strength between the photon and dark photon are set at the level of $10^{-4} - 10^{-3}$ for dark photon masses in the range 0.02 – 10.2 GeV.

Keywords: dark photon, hidden sector, dark matter

New particles neutral under the Standard Model (SM) interactions arise in many models of New Physics [1]. They would only interact weakly with ordinary matter, and could easily have remained undetected thus far. Among the simplest realizations is the existence of a dark sector charged under a new gauge group. The corresponding gauge boson is often referred to as the dark photon (A') and couples to the SM hypercharge via kinetic mixing [2] with a mixing strength ϵ, resulting in an effective interaction between the dark photon and SM fermions. This idea has recently received much attention in the context of dark matter models, where weakly interacting massive particles annihilate into dark photons, which subsequently decay into SM fermions [3, 4, 5]. In this framework, the dark photon mass is constrained to be in the MeV to GeV range [1].

Low-energy e^+e^- colliders offer an ideal environment to probe the existence of dark sectors [6, 7]. Dark photons could be produced in association with a photon in e^+e^- collisions, and decay back to SM fermions. Their width is expected to be well below the experimental resolution, and they could therefore be detected as narrow resonances in radiative $e^+e^- \to \gamma l^+l^-$ ($l = e, \mu$) events. No significant signal for a dark photon has been reported so far, and bounds have been set on the mixing strength between the photon and dark photon as a function of the dark photon mass [8, 9, 10, 11, 12, 13, 14, 15, 16, 17, 18, 19].

A search for dark photon production in the reaction $e^+e^- \to \gamma A', A' \to l^+l^-$ ($l = e, \mu$) has been performed using 514 fb^{-1} of data recorded by the *BABAR* detector [20, 21]. Events with two oppositely charged electrons or muons and a single photon having a center-of-mass (CM) energy greater than 0.2 GeV are selected. Particle identification algorithms and additional kinematic criteria are applied to improve the signal purity. The γl^+l^- system is fitted, constraining the center-of-mass energy of the candidate to be within the beam energy spread and requiring the tracks to originate from the interaction point. The χ^2 of the fit must be less than 30 (for 8 d.o.f). A large contribution from converted photons produced in $e^+e^- \to \gamma\gamma, \gamma \to e^+e^-$ is still present. A neural network is used to remove this background, selecting approximately 70% of the signal while rejecting more than 99.7% of the conversions.

The signal yield as a function of the dark photon mass is extracted by performing a series of fits to the dielectron and the reduced dimuon mass spectra. The reduced dimuon mass, $m_R = \sqrt{m^2_{\mu\mu} - 4m^2_\mu}$, is easier to model near threshold than the dimuon mass. The search is per-

[1] Natural units ($\hbar = c = 1$) are used throughout this letter.

http://dx.doi.org/10.1016/j.nuclphysbps.2015.09.414

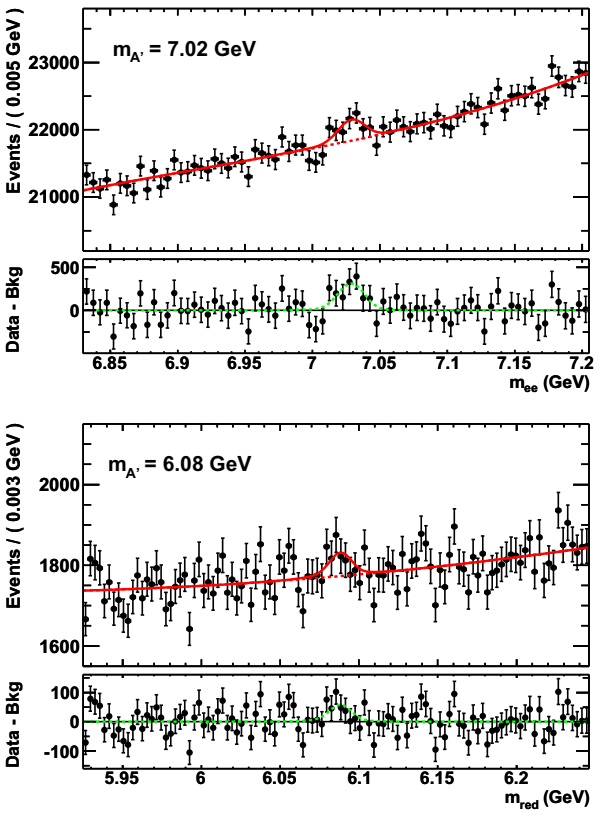

Figure 1: Fit to the dielectron mass (top) and the reduced dimuon mass distribution (bottom) yielding the most significant deviations from zero for each channel. The fit is shown as a solid red line, and the background component as a red dashed line. The difference between the data and the fitted background is shown in the lower panel, together with the fitted signal component (dashed green curve).

formed in steps of approximately half of the dark photon mass resolution, sampling a total of 5704 (5370) mass hypotheses for the dielectron (dimuon) channel. Each fit is performed over a range at least 20 times larger than the corresponding signal resolution, with the constraint $m_{e^+e^-} > 0.015\,\text{GeV}$ for the dielectron channel.

The signal probability density function (pdf) is modeled from simulated signal mass distributions using a non-parametric kernel pdf, and interpolated between the known simulated masses [22]. A sample of $e^+e^- \to \gamma J/\psi\,, J/\psi \to l^+l^-$ events is used to validate the signal resolution predicted by the simulation. We find that the simulation underestimates the dielectron (dimuon) mass resolution by 8% (4%), and we increase the signal pdf width by the corresponding amount. The radiative Bhabha background is described by a third or fourth order polynomial, depending on the mass range, while the radiative dimuon background is parametrized by a third order polynomial, constrained to pass through the origin for fits in the region below 0.05 GeV. Peaking contributions from the $J/\psi\,, \psi(2S)\,, \Upsilon(1S)$, and $\Upsilon(2S)$ resonances are modeled by Crystal Ball functions. The interference between the ω or ϕ resonances with radiative dilepton production is described with an empirical function. We exclude the resonant regions from the search, vetoing ranges of ±30 MeV around the nominal mass of the ω and ϕ resonances, and ±50 MeV around the $J/\psi\,, \psi(2S)$, and $\Upsilon(1S, 2S)$ resonances. Example of fits yielding the most significant signals are shown in Fig. 1. Alternative descriptions of the radiative Bhabha and dimuon contributions based on second or fourth order polynomials are used to assess the uncertainty on the background modeling. This uncertainty is at the level of a few percent for most of the mass hypotheses, but reaches almost 100% (50%) of the statistical uncertainty near $m_{e^+e^-} \sim 20\,\text{MeV}$ (the $\Upsilon(1S, 2S)$ resonances).

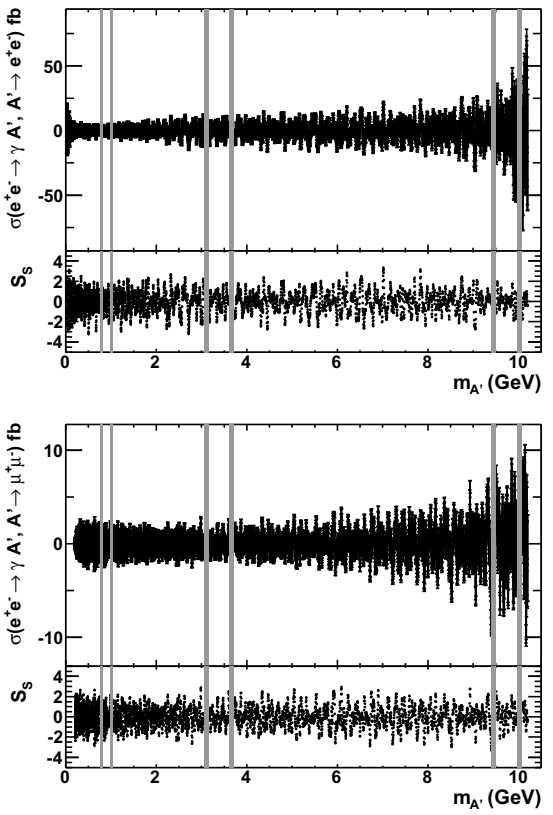

Figure 2: The $e^+e^- \to \gamma A', A' \to e^+e^-$ (top) and $e^+e^- \to \gamma A', A' \to \mu^+\mu^-$ (bottom) cross-sections together with their respective statistical significance (S_S) as a function of the dark photon mass. The gray bands indicate the regions excluded from the analysis.

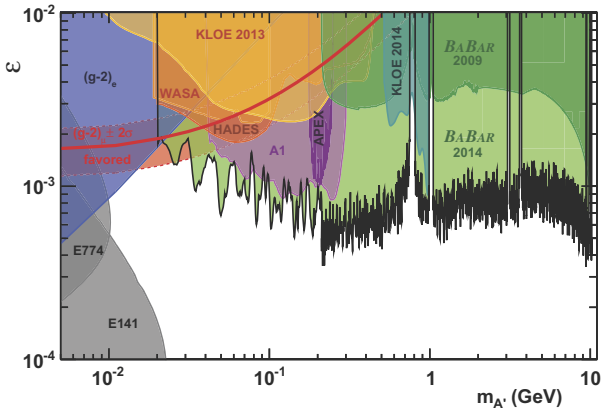

Figure 3: Upper limit (90% CL) on the mixing strength ϵ as a function of the dark photon mass. The values required to explain the discrepancy between the calculated and measured anomalous magnetic moment of the muon [25] are displayed as a red line.

The signal efficiency is estimated from simulated events generated by MadGraph [23]. The detector acceptance and reconstruction efficiencies are determined using a Monte Carlo simulation based on GEANT4 [24]. The efficiency varies between 15%-35%, depending on the dark photon mass and the final state. The bias in the fitted dark photon yields is assessed from a large ensemble of pseudo-experiments and found to be negligible.

The $e^+e^- \to \gamma A', A' \to e^+e^-$ and $e^+e^- \to \gamma A', A' \to \mu^+\mu^-$ cross-sections as a function of the dark photon mass are shown in Fig. 2, together with the statistical significance of each fit. The largest local significance for the dielectron (dimuon) final state is 3.4σ (2.9σ), observed near $m_{A'} = 7.02\,\text{GeV}$ (6.09 GeV). Including trial factors, the corresponding p-value is 0.57 (0.94), consistent with the null hypothesis

We extract the $e^+e^- \to \gamma A'$ cross-section for each final state using the expected dark photon branching fractions $A' \to l^+l^-$ from Ref. [6]. Systematic uncertainties include contributions from the signal and background modeling, the determination of the signal efficiency, the rejection of photon conversions, the dark photon branching fractions, the luminosity, and the limited Monte Carlo statistics. The systematic uncertainty is dominated by the background modeling.

We derive 90% confidence level (CL) Bayesian upper limits on the $e^+e^- \to \gamma A'$ cross-section, assuming a flat prior for the cross-section, and translate these results into 90% CL upper bounds on the mixing strength [7]. Limits at the level of $10^{-4} - 10^{-3}$ for $0.02\,\text{GeV} < m_{A'} < 10.2\,\text{GeV}$ are set, as displayed in Fig 3, significantly improving previous constraints [8, 9, 10, 11, 12, 13, 14, 15, 16, 17, 18, 19]. We further constrain the range of the parameter space favored by interpretations of the discrepancy between the calculated and measured anomalous magnetic moment of the muon [25].

References

[1] See for example R. Essig, J. A. Jaros, W. Wester, P. H. Adrian, S. Andreas, T. Averett, O. Baker and B. Batell *et al.*, arXiv:1311.0029 [hep-ph], and references therein.
[2] B. Holdom, Phys. Lett. B **166**, 196 (1986).
[3] D. P. Finkbeiner and N. Weiner, Phys. Rev. D **76**, 083519 (2007).
[4] M. Pospelov, A. Ritz, and M. B. Voloshin, Phys. Lett. B **662**, 53 (2008).
[5] N. Arkani-Hamed, D. P. Finkbeiner, T. R. Slatyer, and N. Weiner, Phys. Rev. D **79**, 015014 (2009).
[6] B. Batell, M. Pospelov, and A. Ritz, Phys. Rev. D **79**, 115008 (2009).
[7] R. Essig, P. Schuster, and N. Toro, Phys. Rev. D **80**, 015003 (2009).
[8] J. Blumlein and J. Brunner, Phys. Lett. B **701** 155 (2011).
[9] S. Andreas, C. Niebuhr and A. Ringwald, Phys. Rev. D **86**, 095019 (2012).
[10] M. Endo, K. Hamaguchi and G. Mishima, Phys. Rev. D **86**, 095029 (2012).
[11] D. Babusci *et al.* [KLOE-2 Collaboration], Phys. Lett. B **720**, 111 (2013).
[12] D. Babusci *et al.* [KLOE-2 Collaboration], Phys. Lett. B **736**, 459 (2014).
[13] P. Adlarson *et al.* [WASA-at-COSY Collaboration], Phys. Lett. B **726**, 187 (2013).
[14] G. Agakishiev *et al.* [HADES Collaboration], Phys. Lett. B **731**, 265 (2014).
[15] J. Blmlein and J. Brunner, Phys. Lett. B **731** 320 (2014).
[16] H. Merkel, P. Achenbach, C. A. Gayoso, T. Beranek, J. Bericic, J. C. Bernauer, R. Boehm and D. Bosnar *et al.*, Phys. Rev. Lett. **112**, 221802 (2014).
[17] S. Abrahamyan *et al.* [APEX Collaboration], Phys. Rev. Lett. **107**, 191804 (2011).
[18] B. Aubert *et al.* [babar Collaboration], Phys. Rev. Lett. **103**, 081803 (2009).
[19] J. D. Bjorken, R. Essig, P. Schuster and N. Toro, Phys. Rev. D **80**, 075018 (2009).
[20] B. Aubert *et al.* [babar Collaboration], Nucl. Instrum. Meth. A **479**, 1 (2002).
[21] B. Aubert *et al.* [babar Collaboration], Nucl. Instrum. Meth. A **729**, 615 (2013).
[22] A. L. Read, Nucl. Instrum. Meth. A **425**, 357 (1999).
[23] J. Alwall, P. Demin, S. de Visscher, R. Frederix, M. Herquet, F. Maltoni, T. Plehn, and D. L. Rainwater *et al.*, JHEP **0709**, 028 (2007).
[24] S. Agostinelli *et al.* (GEANT4 Collab.), Nucl. Instrum. Methods Phys. Res., Sect. A **506**, 250 (2003).
[25] M. Pospelov, Phys. Rev. D **80**, 095002 (2009).